URSI GASS 2023, Sapporo, Japan, 19 – 26 August 2023

Traveling Ionospheric Disturbances induced by the 2022 Hunga Tonga–Hunga Ha'apai Volcano Eruption

T. C. Liu* [(1)], C. Y. Lin [(1)], J. Y. Liu [(1)], P. H. Lee [(1)], and C. Y. Lin [(1)]
(1) National Central University, Taoyuan, Taiwan; e-mail: veroniqueamberiu@gmail.com; cissi@g.ncu.edu.tw; tigerjyliu@gmail.com; aromatic7777@gmail.com; chiyen.lin1016@gmail.com

Abstract

On 15 January 2022, the Hunga Tonga–Hunga Ha'apai (HTHH) submarine volcano erupted violently, triggering atmospheric waves that perturbed globally, inducing the traveling atmospheric disturbances (TADs) near the Earth's surface and the traveling ionospheric disturbances (TIDs) in the upper atmosphere. In this study, the TADs' propagation is depicted with images of the Himawari-8 satellite. At the same time, ground-based barometers, Doppler sounding systems, and ionosondes are used to observe the TADs and TIDs over Japan and Taiwan. The observation shows that the horizontal speeds of TADs and TIDs vary with altitude. To investigate the features of the observed TIDs, numerical simulations are performed with GITM-R, a three-dimensional non-hydrostatic model for the upper atmosphere equipped with two-way coupling between the coarser-grid layer and the locally refined layer. Finally, the numerical results are compared and discussed with the observation data.

1 Introduction

The eruption of the HTHH submarine volcano (20.54° S, 175.38° W) generated atmospheric pressure disturbances that propagated in the form of Lamb waves, which have been detected globally along with the associated oscillations [1, 2, 3, 4]. Through the images of Himawari-8, the atmospheric Lamb waves are known to arrive in Japan and Taiwan at about 11:10 and 11:30, respectively, followed by the pressure fluctuations recorded by the barometers on the surface. On the other hand, the signals in space are observed about 2 hr before the arrival time depicted by the Homawari-8. The early arrival starting at about 8:10 UT is contributed by electromagnetic conjugacy, mapping the TID reaching Australia to Japan along the conductive magnetic field lines [3, 5].

The ionospheric signatures of natural hazards occurring at the earth's surface provide another view of observation [6] and serve as a possible early warning system [7, 8]. To investigate this unique event, in addition to the Himawari-8 images, the Doppler sounding system in Taiwan, the compressed ionograms, and barometers of both Japan and Taiwan are also used for observation. Furthermore, numerical simulations are conducted with the global ionosphere-thermosphere model with local-grid refinement (GITM-R), focusing on the Tonga near field and the region of east Asia to study the TID and the traveling speeds along the altitude.

2 Methodology

2.1 Observation Datasets

To study the atmospheric perturbation associated with the HTHH eruption, the Himawari-8 images are used to observe TADs of upper-level tropospheric water vapor at about 8.2 km altitude with the wavelength of 6.2 μm infrared band (spatial resolution of 2 km; time resolution of 10 minutes). In addition, the Doppler shift spectrograms recorded in Taiwan, the compressed ionograms from the ionosonde stations, and the air pressure records from Japan Meteorological Agency and the 10m-tower of National Central University, which are co-located to the ionosonde stations, are implied to observe the TADs and TIDs over Taiwan and Japan. The locations of the HTHH volcano, barometers, ionosondes, as well as the Doppler sounding systems are shown in Figure 1.

2.1 Observation Datasets

GITM is a three-dimensional model for Earth's thermosphere and ionosphere that self-consistently solves the neutral, ion, and electron temperature in the spherical coordinate system [9, 10, 11]. Furthermore, for the high temporal-spatial resolution computational demands of the upper atmosphere modeling, GITM-R is developed with the two-way coupling between the coarser-grid layer and the locally refined layer [12, 13]. This study performs numerical simulations with GITM-R in three and two layers. The resolution and domain settings of the simulations are shown in Figure 2 and Table 1. The altitudinal domain extended from 100 to 600 km with a vertical resolution of one-third of the scale height. The perturbation is designed with the Himawari-8 observation and inputted at the lower boundary. The numerical scenarios of 15 January 2022 without the HTHH atmospheric perturbation are also conducted to study the direct effect of the traveling atmospheric waves.

3 Result

The TIDs observed by the ionosondes lead the air pressure jumps recorded near the surface by about 2 hours. The

This paper's copyright is held by the author(s). It is published in these proceedings and included in any archive such as IEEE Xplore under the license granted by the "Agreement Granting URSI and IEICE Rights Related to Publication of Scholarly Work."

horizontal TAD speed in Himawari-8 images is about 310 m/s, while the one obtained with ground pressure is about 296.9 m/s over Japan and Taiwan during 11:10-12:10 UT. The averaged horizontal TID speeds observed by the Doppler sounding systems and ionosondes are respectively about 451.2 and 525.1 m/s, which fall in the range of sound speed in the ionosphere computed from the NRLMSISE-00 model on 15 January 2022 at 9:00 UT (17:00 Local Time) above Taiwan.

Numerical results show that the TIDs travel in the HTHH near field with speeds of about 310.5 m/s and 366.67 m/s at 200 km and 300 km, respectively [Fig. 3]. As the TIDs propagate to Japan and Taiwan, which locating in the far-field region, the TIDs travel with an average speed of 365 m/s at 300 km [Fig.4]. In addition, significant irregularities at 300 km altitude are observed following the TIDs, and they could also be found with the variation of total electron content (TEC) at the low latitude as well. This numerical finding agrees with the studies of the equatorial plasma bubble triggered by the HTHH eruption [14, 15, 16].

4 Discussion

The early arrival of the TIDs from the observation data, though it corresponds to the sound speed profile, could not be ruled out that it is contributed by the electromagnetic conjugacy. Nevertheless, the profile figures of the electron density of the numerical studies support that TIDs observed at higher altitudes arrive earlier than the lower ones. The simulation results show that the TIDs travel at speeds of about 365 m/s at 300 km and 328 m/s at 200 km in the study region. The TEC variations in the far-fields region show strong irregularities at the low latitude, which could be caused by the increased vertical plasma transport triggered by the TIDs.

5 Figures and Tables

5.1 Figures

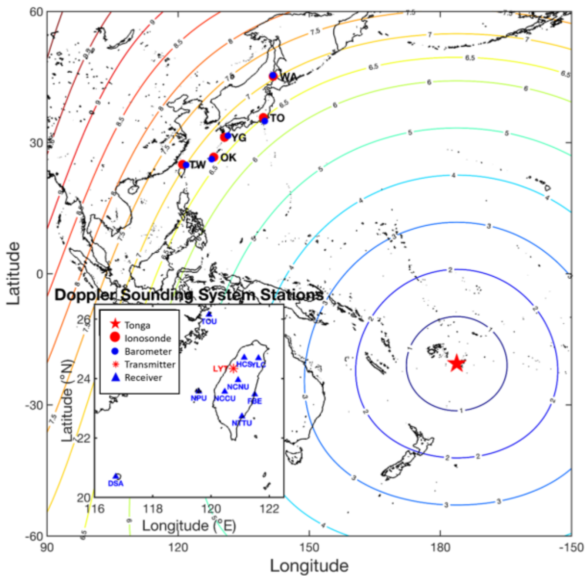

Figure 1. Locations of the Tonga volcano, barometers, ionosondes, and the Doppler sounding systems in Taiwan and Japan. Colored curves stand for the travel time of TADs in Himawari-8 images.

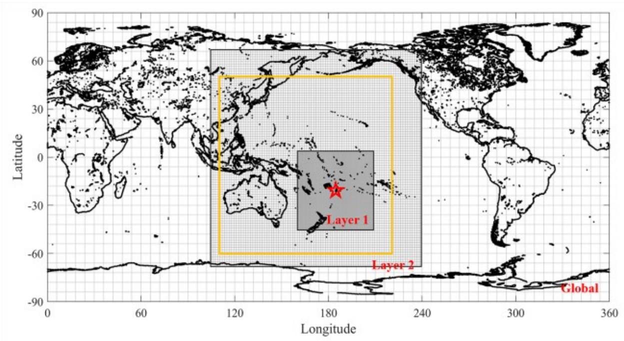

Figure 2. Numerical domains of the three-layer and two-layer GITM-R simulations. The star sign denoted the location of the HTHH volcano. The local region of the two-layer simulation is shown with the yellow square, covering 110°×110° in latitude and longitude.

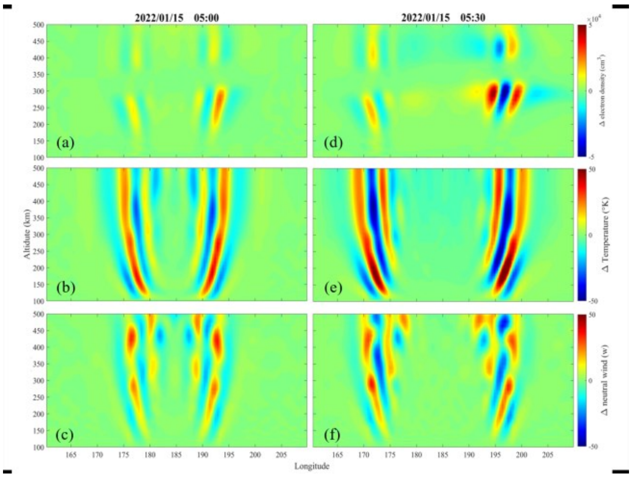

Figure 3. Near-field electron density (a, d), temperature (b, e), and neutral wind (c, f) variations are plotted as a function of longitude and altitude at 20.54°S at 05:00 UT and 05:30 UT.

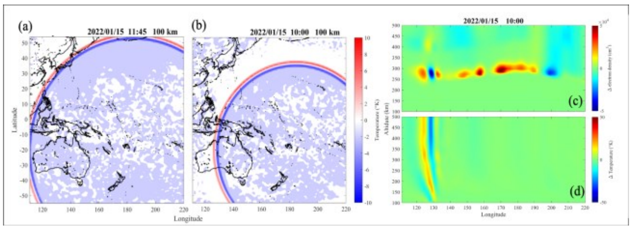

Figure 4. TIDs in the HTHH far field. (a, b) Snapshots of the temperature perturbations at the lower boundary (100 km) at 11:45 and 10:00. The far-field electron density (c) and the temperature variations (d) are shown as a function of longitude and altitude at 20.54°S 10:00 UT.

5.2 Tables

Table 1 Setting of the GITM-R numerical layers

Simulation	Layer	Resolution	Simulation Domain
Three-Layer	1	0.5°×0.5°	-45.57°-4.43° 159.62°-209.62°
	2	1.5°×1.5°	-68.07°-66.93° 104.62°-239.62°
	Global	6°×6°	-90°-90° 0°-360°
Two - Layer	Local	1°×1°	-55.57°-54.43° 109.62°-219.62°
	Global	3.5°×4°	-90°-90° 0°-360°

Acknowledgements

This study is supported by the National Science and Technology Council (MOST110-2111-M-008-034-MY2; MOST111-2111-M008-018).

References

[1] D. Adam, "Tonga volcano eruption created puzzling ripples in Earth's atmosphere," *Nature*, **601**, January 2022, pp. 497, doi: 10.1038/d41586-022-00127-1.

[2] T. Kubota, T. Saito, and K. Nishida, "Global fast-traveling tsunamis driven by atmospheric Lamb waves on the 2022 Tonga eruption," *Science*, **377**, 6601, May 2022, pp. 91-94, doi: 10.1126/science.abo4364.

[3] J. T. Lin, P. K. Rajesh, C. C. Lin, M. Y. Chou, J. Y. Liu, J. Yue, T. Y. Hsiao, H. F. Tsai, H. M. Chao, M. H. Kung, "Rapid conjugate appearance of the giant ionospheric Lamb Wave signatures in the Northern Hemisphere after Hunga-Tonga Volcano eruptions," *Geophys Res Lett*, **49**, April 2022, 2022GL098222, doi: doi:10.1029/2022GL098222.

[4] S. R. Zhang, J. Vierinen, E. Aa, L. P. Goncharenko, P. J. Erickson, W. Rideout, A. J. Coster, and A. Spicher, "Tonga volcanic eruption induced global propagation of ionospheric disturbances via Lamb waves," *Front. Astron. Space Sci*, **9**, March 2022, pp. 1-59, doi: 10.3389/fspas.2022.871275.

[5] A. Shinbori, Y. Otsuka, T. Sori, M. Nishioka, S. Perwitasari, T. Tsuda, and N. Nishitani, "Electromagnetic conjugacy of ionospheric disturbances after the 2022 Hunga Tonga-Hunga Ha'apai volcanic eruption as seen in GNSS-TEC and SuperDARN Hokkaido pair of radars observations," *Earth, Planets and Space*, **74**, 106, July 2022, pp. 1-17, doi: 10.1186/s40623-022-01665-8.

[6] E. Astafyeva, "Ionospheric detection of natural hazards," *Rev. Geophys.*, **57,** 4, December 2019, pp. 1265-1288. doi: 10.1029/2019RG000668.

[7] M. Kamogawa, Y. Orihara, C. Tsurudome,Y. Tomida, T. Kanaya, D. Ikeda, A. R. Gusman, Y. Kakinami, J. Y. Liu, and A. Toyoda, "A possible space-based tsunami early warning system using observations of the tsunami ionospheric hole," *Sci. Rep*., **6**, December 2016, 37989, doi: 10.1038/srep37989.

[8] J. Y. Liu, C. Y. Lin, Y. L. Tsai, T. C. Liu, K. Hattori, Y. Y. Sun, and T. R. Wu, "Ionospheric GNSS total electron content for tsunami warning," *J. Earthq. Tsunami.*, **13**, August 2019, 1941007, doi: 10.1142/s1793431119410070.

[9] A. Ridley, Y. Deng, and G. Toth, "The Global Ionosphere–Thermosphere Model," *J Atmos Sol Terr Phys*, **68**, 8, May 2006, pp. 839-864, doi: 10.1016/j.jastp.2006.01.008.

[10] C. Y. Lin, Y. Deng, and A Ridley, "Atmospheric gravity waves in the ionosphere and thermosphere during the 2017 solar eclipse," *Geophys Res Lett,* **45**, 11, April 2018, pp. 5246-5252, doi: 10.1029/2018GL077388.

[11] C. Y. Lin, Y. Deng, K. Venkataramani, J. Yonker, and S. M. Bailey, "Comparison of the thermospheric nitric oxide emission observations and the GITM simulations: Sensitivity to solar and geomagnetic activities," J. Geophys. Res. Space Phys, **123**, 12, September 2018, pp. 10239-10253, doi: 10.1029/2018JA025310.

[12] Y. Deng, Q. Zhu, C. Y. Lin, M. Jin, C. Liu, and C. Sheng, "Electric field variability and impact on the ionosphere-thermosphere," in Cross-scale Coupling and Energy Transfer in the Magnetosphere-Ionosphere-Thermosphere System, Y. Nishimura, O. Verkhoglyadova, Y. Deng, S. R. Zhang, Amsterdam: Elsevier, 2021, pp. 17-33.

[13] Y. Zhao, Y. Deng, J. S. Wang, S. R. Zhang, C. Y. Lin, "Tropical cyclone-induced gravity wave perturbations in the upper atmosphere: GITM-R simulations," J Geophys Res Space Phys, **125**, June 2020, e2019JA027675, doi: 10.1029/2019JA027675.

[14] E. Aa, S. R. Zhang, P. J. Erickson, J. Vierinen, A. J. Coster, L. P. Goncharenko, A. Spicher, and W. Rideout, "Significant ionospheric hole and equatorial plasma bubbles after the 2022 Tonga volcano eruption," *Space Weather*, **20**, 7, June 2022, p.e2022SW003101, doi: 10.1029/2022SW003101.

This paper's copyright is held by the author(s). It is published in these proceedings and included in any archive such as IEEE Xplore under the license granted by the "Agreement Granting URSI and IEICE Rights Related to Publication of Scholarly Work."

[15] P. K. Rajesh, C. C. H. Lin, J. T. Lin, C. Y. Lin, J. Y. Liu, T. Matsuo, C. Y. Huang, M. Y. Chou, J. Yue, M. Nishioka, and H. Jin, H, ”Extreme Poleward Expanding Super Plasma Bubbles Over Asia-Pacific Region Triggered by Tonga Volcano Eruption During the Recovery-Phase of Geomagnetic Storm,” *Geophys Res Lett,* **49**, 15, August 2022, e2022GL099798, doi: 10.1029/2022GL099798.

[16] J. D. Huba, E. Becker, and S. L. Vadas, “Simulation Study of the 15 January 2022 Tonga Event: Development of Super Equatorial Plasma Bubbles,” *Geophys Res Lett,*, **50**, December 2022, e2022GL101185.